Available online at www.sciencedirect.com
ScienceDirect
Journal of Solid State Chemistry 180 (2007) 3529–3534
JOURNAL OF SOLID STATE CHEMISTRY
www.elsevier.com/locate/jssc

Morphology-dependent photoluminescence property of red-emitting *Ln*OCl:Eu (*Ln* = La and Gd)

Seoung-Soo Lee, Ho-In Park, Chung-Hyung Joh, Song-Ho Byeon*

College of Environment and Applied Chemistry, Kyung Hee University, Kyung Ki 446-701, Republic of Korea

Received 9 July 2007; received in revised form 23 September 2007; accepted 19 October 2007
Available online 23 October 2007

Abstract

Three different synthetic methods, the liquid phase process in HCl solution, the solvothermal reaction, and the surfactant-assisted solvothermal reaction, were explored to selectively control the particle shape and to enhance the luminescence intensity of the PbFCl-type red-emitting oxychloride phosphors *Ln*OCl:Eu (*Ln* = La and Gd). The solvothermal pressure facilitated the low-temperature crystallization of the rod-shape particles for both *Ln* = La and Gd. It is noted that LaOCl:Eu nanorods show highly porous particle surface and quite low photoemission intensity. In contrast, the solvothermal synthesis could highly enhance the red-emission of GdOCl:Eu with no porous surface so as to be comparable to that of commercial Y_2O_3:Eu phosphor. An addition of surfactant material during solvothermal reaction yielded a rhomboidal-shape phosphor particles with no porous surface for both *Ln* = La and Gd. Interestingly, the elimination of surface porosity by using a surfactant significantly increased the emission intensity of LaOCl:Eu. It is proposed that the application of solvothermal technique for the synthesis of the PbFCl-type oxychloride phosphors is very effective to selectively control the particle shape and consequently to enhance the photoemission intensity if we use an appropriate surfactant material.

Keywords: Phosphors; Oxychlorides; Solvothermal; Luminescences; Morphology

1. Introduction

Luminescent phosphors of oxides, halides, and oxyhalides of lanthanides are of interest for displays, up-conversion lasers, and other related optoelectronic devices [1–4]. For instance, Y_2O_3:Eu and $NaYF_4$:Yb, Er are well-known UV-excited and IR-excited phosphors, respectively [5]. Up-conversion from IR radiation to visible light or ultraviolet radiation has been reported for several rare earths, Pr^{3+}, Eu^{3+}, Er^{3+}, Ho^{3+}, and Tm^{3+} in many oxides, halides, and oxyhalide matrices [6–8]. Such studies have been focused to develop the solid-state up-conversion lasers based on rare earth-doped bulk materials and fibers. Lanthanum oxychloride (LaOCl) and gadolinium oxychloride (GdOCl) doped with Eu^{3+}, Tb^{3+}, and Tm^{3+} exhibit strong UV and cathode-ray excited red-, green-, and blue-luminescences, respectively, which are useful in lamp and display applications [9,10]. The solid-solution, $La_{1-x}Gd_xOCl$:Eu, was investigated to improve the luminescent properties for applications in displays and X-ray intensifying screens [11]. Up-conversion luminescence of Sm^{3+} in GdOCl was also observed in the Raman spectrum of GdOCl:Sm [12]. Ca-doped LaOCl has shown a potential application for the water-insoluble solid electrolyte with high Cl^- ion conductivity [13,14].

In contrast to typical two-dimensional characteristics of other *MOX*-families (*M* = transition metals and small lanthanides, *X* = halides), the structure of PbFCl-type lanthanide oxyhalides is practically three-dimensional [15]. Because this structure is not active to the host–guest reactions, such type of oxychlorides have not been actively investigated. Conventional preparation of *Ln*OCl (*Ln* = large lanthanides) with the PbFCl-structure employs two solid-state processes. One method includes the calcination of the mixture of Ln_2O_3 and excess NH_4Cl followed by recrystallization at high temperature (900 °C) in N_2 gas flow [16,17]. The other procedure is composed of

*Corresponding author. Fax: +82 31 202 7337.
E-mail address: shbyun@khu.ac.kr (S.-H. Byeon).

0022-4596/$ - see front matter © 2007 Elsevier Inc. All rights reserved.
doi:10.1016/j.jssc.2007.10.020

the heat treatment (700 °C) of $LnCl_3$ with $CaCl_2$ as a flux [18]. In an attempt to induce the controllable isotropic and anisotropic morphologies at lower temperatures, three different methods were explored to prepare the powder samples of *Ln*OCl:Eu (*Ln* = La and Gd) in the present work. Interestingly, quite different photoemission intensities were observed depending on the morphology and the surface structures of *Ln*OCl:Eu particles. In particular, the solvothermal synthesis could highly enhance the red-emission intensity of GdOCl:Eu to be comparable to that of commercial Y_2O_3:Eu phosphor. In this paper, we compared the photoemission behavior of *Ln*OCl:Eu (*Ln* = La and Gd) phosphors as a function of particle morphology which is strongly dependent on the synthetic conditions.

2. Experimental

The general composition, *Ln*OCl:Eu (*Ln* = La and Gd) containing 10 mol% Eu^{3+} ions or $Ln_{0.90}Eu_{0.10}OCl$, was examined in this study. The first synthetic method was based on the liquid phase process. Stoichiometric amounts of Ln_2O_3 and Eu_2O_3 were dissolved in small amount of HCl solution. The resulting solution was stirred for 1 h, evaporated, and dried in vacuum. The obtained powder was finally heated at 500 °C for 10 h. To induce a rather anisotropic morphology, the solvothermal process was adopted to synthesize *Ln*OCl:Eu for the second method. About 5.2 mmol of $LaCl_3 \cdot 7H_2O$ and 0.58 mmol of $EuCl_3 \cdot 6H_2O$ or 4.8 mmol of $GdCl_3 \cdot 6H_2O$ and 0.53 mmol of $EuCl_3 \cdot 6H_2O$ were dissolved in 30 mL of absolute ethanol for LaOCl:Eu or GdOCl:Eu, respectively. Each solution was put into a Teflon-lined stainless steel autoclave with a capacity of 40 mL at room temperature. The solution was then stirred vigorously before the autoclave was sealed and maintained at 120–130 °C for 12 h. After the reaction was completed, the resulting solid product was collected by filtration, washed with absolute ethanol, dried at room temperature, and then heated at 500 °C for 10 h. The third method included a surfactant-assisted solvothermal reaction. 5.2 mmol of $LaCl_3 \cdot 7H_2O$, 0.58 mmol of $EuCl_3 \cdot 6H_2O$, and 7.8 mmol of sodium oleate were dissolved in a mixture solvent composed of 5.2 mL absolute ethanol, 3.9 mL distilled water, and 9.1 mL *n*-hexane (volume ratio = 4:3:7). In case of GdOCl:Eu, 4.8 mmol of $GdCl_3 \cdot 6H_2O$, 0.53 mmol of $EuCl_3 \cdot 6H_2O$, and 7.2 mmol of sodium oleate were dissolved in a mixture solvent composed of 4.8 mL absolute ethanol, 3.6 mL distilled water and 8.4 mL *n*-hexane (volume ratio = 4:3:7). The resulting solution was refluxed at 70–80 °C for 4 h, put into a Teflon-lined stainless steel autoclave and then maintained at 120–130 °C for 12 h. After the reaction was completed, the resulting solid product was collected by filtration, washed with absolute ethanol, dried at room temperature, and then heated at 500 °C for 12 h.

The powder X-ray diffraction (XRD) patterns were recorded on a rotating anode installed diffractometer (18 kW). The Cu$K\alpha$ radiation used was monochromated by a curved-crystal graphite. Field emission scanning electron microscopy (FE-SEM) was carried out with a Zeiss LEO SUPRA 55 electron microscope operating at 10 kV. Energy-dispersive X-ray (EDX) analysis was also used to characterize the samples imaged by FE-SEM. Specimens for electron microscope were coated with Pt for 200 s under vacuum. The photoluminescence (PL) intensity of phosphors was measured at room temperature using a Hitachi F-4500 spectrophotometer with a Xenon flash lamp. The sample loaded on a powder holder provided by Hitachi was mounted about 45° to the excitation source for PL measurement. All samples were analyzed with the same weight and the same slit was used to measure the excitation and emission spectra. The excitation spectra were measured at the emission wavelength of 617 nm (LaOCl:Eu) and 619 nm (GdOCl:Eu) with maximum intensity. The emission spectra were recorded using maximum excitation wavelength. For comparison, the photoemission spectrum of commercial Y_2O_3:Eu (λ_{ex} = 262 nm) was measured on the same condition.

3. Results and discussion

The oxychlorides of yttrium, bismuth, and the large lanthanides crystallize in the tetragonal PbFCl-structure (space group *P*4/*nmm*) [16]. The idealized structure of *Ln*OCl (*Ln* = La and Gd) is represented as an example in Fig. 1. Overall structure comprises distinct covalent $(LnO)^+$ cation and Cl^- anion layers perpendicular to the *c*-axis of the unit cell. In this structure, the Ln^{3+} ions occupy the distorted square antiprismatic sites on both sides of the central oxide sheet so that they are coordinated

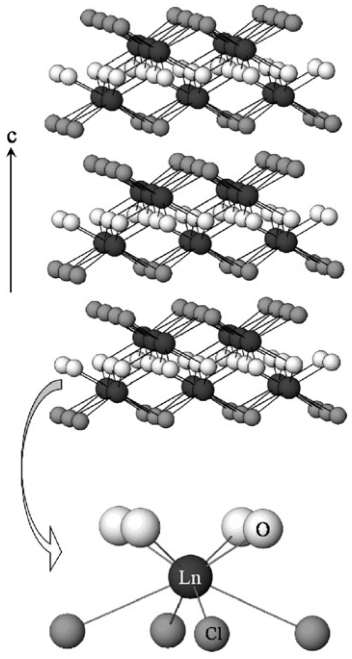

Fig. 1. Idealized PbFCl-type structure of *Ln*OCl.

to four oxygen ions and four chloride ions. An additional chloride in adjacent layer caps the four-chloride face of the square antiprism. This structure accordingly has no true van der Waals gap between layers. Because of such structural characteristics, no topochemical reaction has been reported for *Ln*OCl with the PbFCl-structure.

Heat treatment at 400 °C was sufficient for the crystallization of *Ln*OCl:Eu phosphor in three different processes explored in the present work. This temperature is quite low in comparison with 700–900 °C for conventional preparation methods of the PbFCl-type *Ln*OCl. High degree of mixing of each components on an atomic level in the liquid phase is primarily responsible for the lowering of formation temperature of *Ln*OCl:Eu. The solvothermal pressure would also facilitate the crystallization at lower temperature. However, the final heat treatment was carried out at 500 °C for all compounds in this work to achieve the optimal PL emission intensity. The structure and morphology of the obtained *Ln*OCl:Eu phosphors were collapsed to form Ln_2O_3:Eu oxide phosphors above 700 °C. To develop the surfactant-assisted solvothermal method, several attempts were made with different surfactants. The morphology of *Ln*OCl:Eu phosphor could be selectively controlled when we used the sodium oleate to avoid a particle growth to the rod-shape during solvothermal reaction. When we applied these procedures to prepare the PbFCl-type *Ln*OCl with different lanthanide activators or without any activator, similar behavior was observed in the synthesis. It is accordingly proposed that the present synthetic methods would be also effective for the improvement of oxychloride up-conversion lasers or Cl^- ion conducting solid electrolytes.

The XRD patterns of *Ln*OCl:Eu (*Ln* = La and Gd) phosphors prepared by the liquid phase reaction, the solvothermal reaction, and the surfactant-assisted solvothermal reaction are compared in Fig. 2. All of the diffraction peaks for both LaOCl:Eu and GdOCl:Eu can be indexed to the tetragonal PbFCl-structure, which are in good agreement with the structure data in literatures [19,20]. Based on the full-width at half-maximum (FWHM) of diffraction peaks shown in this figure, no significant difference in crystallinity of *Ln*OCl:Eu phosphors is induced regardless of the adopted synthetic methods.

To gain an insight into the influence of particle shape and size on the luminescence characteristics of LaOCl:Eu phosphor, we have compared the FE-SEM images of the specimens obtained by three different synthetic methods in Fig. 3. It can be seen from the photographs that the reaction in HCl solution followed by the heat treatment at 500 °C results in strongly agglomerated particles with no distinguishable shape and size distribution (Fig. 3a). In contrast, the application of solvothermal process produces typical nanorods of a few μm in length and 200–300 nm in diameter (Fig. 3b). Most of nanorods are inclined to align parallel to the rod axis and form a straight bundle structure. It is noted that the surface of LaOCl:Eu nanorods is highly porous as shown in the inset of

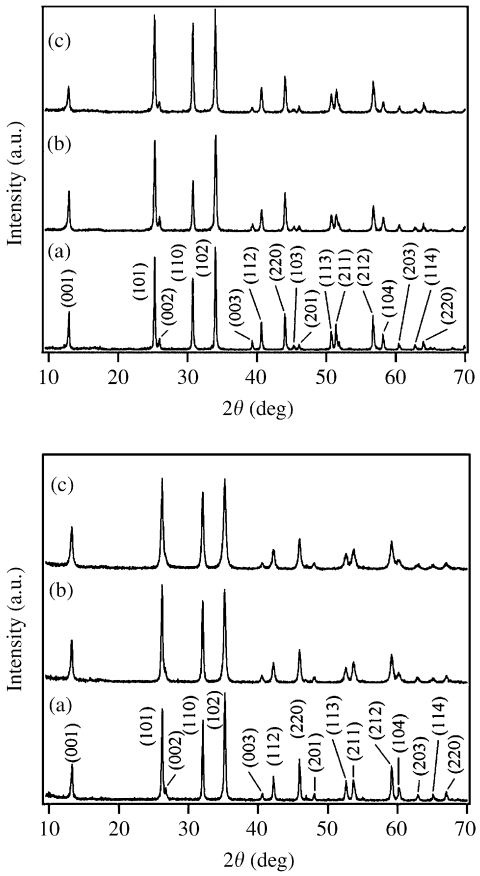

Fig. 2. X-ray diffraction patterns of (top) LaOCl:Eu and (bottom) GdOCl:Eu prepared by (a) liquid-phase reaction, (b) solvothermal reaction, and (c) surfactant-assisted solvothermal reaction.

Fig. 3b. Because of such high porosity, the minimized surface energy could be achieved by the surface to surface assembling of the nanorods. The origin of high porosity is not straightforward. If the individual rods are not single crystalline, the post-heat treatment at 500 °C would induce an irregular particle contraction for the crystallization of LaOCl with an anisotropic structure. Because of weak photoemission intensity of this porous rod-shape phosphor (as will be discussed in the next part), the sodium oleate was added to avoid a particle growth to the rod-shape during solvothermal reaction and to avoid the formation of porous surface after the post-heat treatment. Such a surfactant-assisted solvothermal reaction yielded the phosphor particles with quite different morphology from that prepared without surfactant. As shown in Fig. 3c, the particle morphology is a rhomboidal-shape rather than a rod-shape and the microstructure of particle surface is not porous. This result indicates that, in the presence of an appropriate surfactant, the growth of particles could be controlled and consequently less aggregation and narrower size and shape distributions could be induced by the solvothermal reaction.

A broad maximum centered at around 300 nm and a sharp one at 394–396 nm were observed in the excitation spectra of LaOCl:Eu phosphors. This behavior is

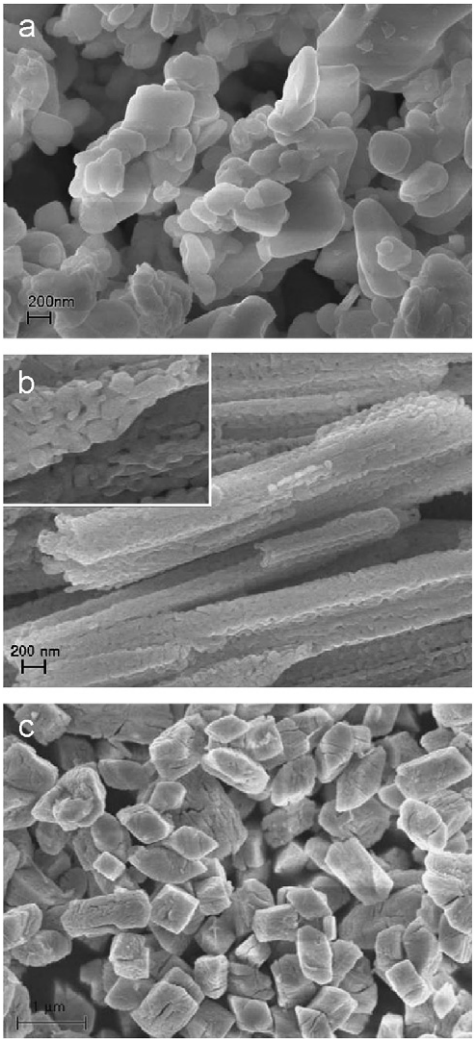

Fig. 3. SEM photographs of LaOCl:Eu prepared by (a) liquid-phase reaction (bar = 200 nm), (b) solvothermal reaction (bar = 200 nm, the inset is the enlarged image showing porous surface.), and (c) surfactant-assisted solvothermal reaction (bar = 1 μm).

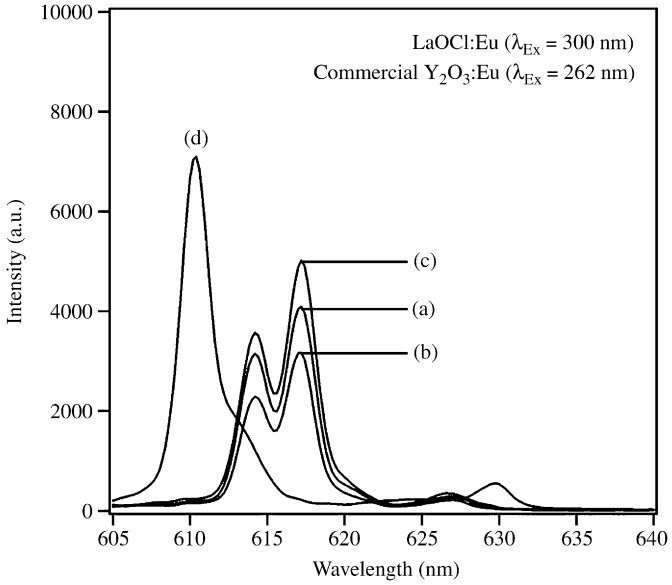

Fig. 4. Comparison of photoemission spectra of LaOCl:Eu prepared by (a) liquid-phase reaction, (b) solvothermal reaction, and (c) surfactant-assisted solvothermal reaction with that (d) of commercial Y_2O_3:Eu phosphor.

consistent with the previous literature data [21]. Therefore, the photoemission spectra were recorded with the excitation wavelength of 300 nm. In Fig. 4, the PL emission spectra of LaOCl:Eu phosphors are compared with that of commercial red-phosphor Y_2O_3:Eu. The strong red-emissions at 610–630 nm is associated with $^5D_0 \rightarrow {}^7F_2$ transition of Eu^{3+}, which is divided into three components at ~614, ~617, and ~627 nm by the crystal field splitting. The position and relative intensity of these components are slightly variable depending on the nature and composition of Pb sites in the PbFCl-structure [9,11,21]. As shown in this figure, it is apparent that the relative emission intensities are considerably different from one another depending on the preparation conditions of LaOCl:Eu.

Because of the strong agglomeration, irregular shape, and poor size distribution of particles (Fig. 3a), the PL emission intensity of LaOCl:Eu phosphor prepared by the liquid phase method in HCl solution is much lower than that of commercial Y_2O_3:Eu (Fig. 4a). One interesting feature is that an adoption of solvothermal technique to improve the shape and size distribution of particles resulted in a significantly different luminescence intensity before and after the addition of surfactant material. When the sodium oleate was not added during solvothermal reaction, the resulting LaOCl:Eu phosphor exhibits much weaker emission intensity in comparison with that prepared by the liquid phase procedure (Fig. 4b). If we consider the morphology of corresponding phosphor particles shown in Fig. 3b, the significantly reduced PL intensity would be associated with the microstructure of particle surface. It is generally accepted that the porous surface could increase the effectiveness of absorption and consequently enhance the emission intensity because of the larger irradiated surface area. In this respect, the low emission intensity and the high porosity of LaOCl:Eu phosphor seems to contradict each other. However, the number of surface defects would be also increased by the highly porous surface and the accompanied enlargement of surface area of particles. If these defects act as nonradiative recombination centers, the emission intensity of porous rod-shape particles would be reduced despite the large surface area. When we added the sodium oleate as a surfactant to avoid the formation of porous surface, a considerable increase in emission intensity was observed for the obtained LaOCl:Eu phosphor. As shown in Fig. 4c, the relative intensity is close to 150% in comparison with that of phosphor prepared without surfactant. Considering the particle shape and surface with no porosity (Fig. 3c), it is demonstrated that the concentration and the number of surface defects are crucial for the determination of PL efficiency of LaOCl:Eu phosphor. These results indicate that the application of solvothermal technique for the synthesis of LaOCl:Eu is

very effective to selectively control the particle shape and consequently to enhance the photoemission intensity if we use an appropriate surfactant.

GdOCl:Eu phosphor prepared in this work also showed quite different morphologies depending on the experimental conditions. Fig. 5a is the FE-SEM image of GdOCl:Eu prepared by the liquid phase reaction in HCl solution followed by the heat treatment at 500 °C. Compared with LaOCl:Eu prepared under the same condition (Fig. 3a), GdOCl:Eu shows better size and shape distribution of rounded-shape nanoparticles. The size of particles is close to 50–100 nm. In Fig. 5b, GdOCl:Eu prepared under the solvothermal condition shows relatively regular and rigid rod-shape particle morphology. In contrast to LaOCl:Eu particles prepared under the solvothermal condition (Fig. 3b), the surface structure of rod-shape particles of GdOCl:Eu is not porous and any behavior to align parallel to the rod axis is not observed between particles. This image suggests that no porous surface results in the surface energy low enough to be stable without surface-to-surface assembling of rod-shape particles. Multiple attempts to induce a porous surface as in LaOCl:Eu were unsuccessful. The shape of GdOCl:Eu particles prepared by the surfactant-assisted solvothermal reaction is similar to that of LaOCl:Eu (Fig. 3c). Instead of rigid rod-shape particles prepared without any surfactant, the rhomboidal particles with no porous surface are seen in Fig. 5c. No aggregation is observed between particles. Thus, it is evident that the solvothermal condition facilitates the particle growth and an addition of appropriate surfactant can control the direction of particle growth in the synthesis of PbFCl-type oxychlorides.

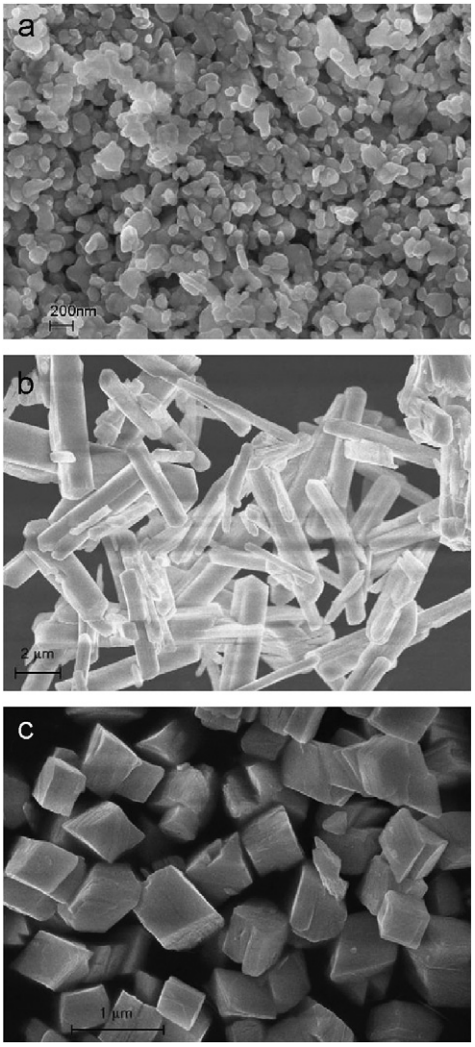

Fig. 5. SEM photographs of GdOCl:Eu prepared by (a) liquid-phase reaction (bar = 200 nm), (b) solvothermal reaction (bar = 2 μm), and (c) surfactant-assisted solvothermal reaction (bar = 1 μm).

Several repeated measurements of the emission spectra of GdOCl:Eu phosphors showed a strong dependence of relative intensity on the particle morphology, which is similar to the behavior observed in LaOCl:Eu. Fig. 6 compares the PL emission spectra of commercial Y_2O_3:Eu with those of GdOCl:Eu as a function of synthetic conditions. Because a broad maximum centered at around 300 nm was observed in the excitation spectra, the photoemission spectra were recorded with the excitation wavelength of 300 nm. The strong red-emission at 610–630 nm and the splitting into three components at ~614, ~619, and ~629 nm are in agreement with typical spectra of *Ln*OCl:Eu (*Ln* = Y, La, Gd) red-phosphors [9,11,21]. It can be seen in this figure that overall emission intensities of GdOCl:Eu are higher than those of LaOCl:Eu when they are prepared along the same procedures (Fig. 4). Based on the emission intensity relative to that of commercial Y_2O_3:Eu, GdOCl:Eu prepared by the liquid phase method in HCl solution (Fig. 6a) exhibits more intense emission than LaOCl:Eu prepared under the same condition. Of the most interest to us is that the emission

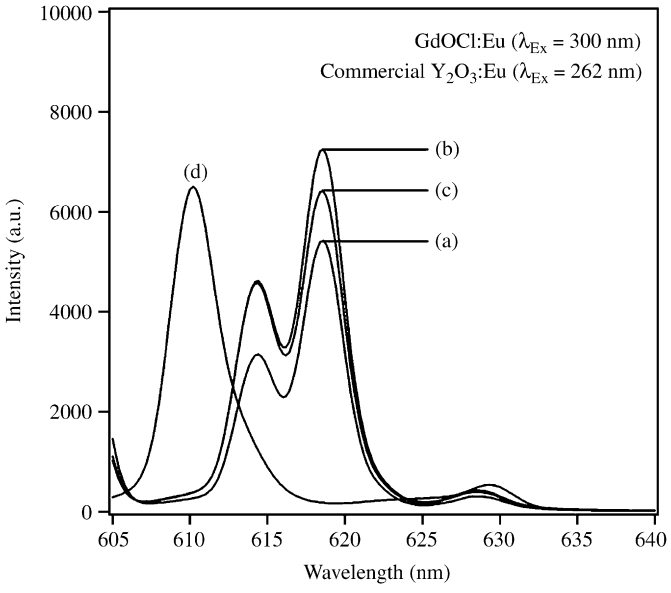

Fig. 6. Comparison of photoemission spectra of GdOCl:Eu prepared by (a) liquid-phase reaction, (b) solvothermal reaction, and (c) surfactant-assisted solvothermal reaction with that (d) of commercial Y_2O_3:Eu phosphor.

intensity of GdOCl:Eu prepared by the solvothermal reaction is superior than that of Y_2O_3:Eu as shown in Fig. 6b. This behavior is completely different from a significant decrease in emission intensity of LaOCl:Eu when prepared by the same procedure. The existence of OH impurity in the particle surface could affect the PL efficiency. However, the dehydroxylation of the *Ln*OCl particle surface occurs at about 380 °C [22,23]. Since the *Ln*OCl:Eu phosphors were obtained after heat treatment at 500 °C in the present work, the existence of OH impurity could be ruled out. Indeed, no noticeable difference was observed when the measurements of IR spectra were carried out for the sample powders. If we consider the highly porous surface of solvothermally prepared LaOCl:Eu nanorods, it would be suggested that no porous surface is responsible for the highly enhanced emission of GdOCl:Eu nanorods. In contrast, an addition of surfactant material during solvothermal process plays no great role to enhance the emission intensity of GdOCl:Eu phosphor with no porous surface (Fig. 6c) despite the resulting particles show completely different shape (Fig. 5c). Thus, a decrease in emission intensity by an increase of the number of surface defects (i.e. nonradiative recombination centers) seems to be predominant on an increase in absorption efficiency by larger irradiated surface area with increasing porosity.

4. Conclusion

In an attempt to induce the controllable isotropic and anisotropic morphologies of *Ln*OCl:Eu (*Ln* = La and Gd) phosphors, three different methods, the liquid phase process in HCl solution, the solvothermal reaction, and the surfactant-assisted solvothermal reaction, were explored at lowered temperatures. It is evident from FE-SEM images that the solvothermal condition strongly influence on the particle growth at low temperature and an addition of appropriate surfactant can control the direction of growth in the synthesis of PbFCl-type oxychlorides. If we correlate the particle shape, the surface structure, and the PL behavior, it is suggested that the microstructure of particle surface should be improved for the high enhancement of UV-excited PL efficiency of *Ln*OCl:Eu (*Ln* = La and Gd) phosphors. Further investigation should be carried out for understanding the effect of solvothermal synthesis on the IR-excited up-conversion behaviors of GdOCl:*Ln* (*Ln* = lanthanides).

Acknowledgment

This work was supported by the KOSEF through Grant R01-2004-000-10610-0.

References

[1] C. Adachi, M.A. Baldo, M.E. Thompson, S.R. Forrest, J. Appl. Phys. 90 (2001) 5048.
[2] G. Yi, B. Sun, F. Yang, D. Chen, Y. Zhou, J. Cheng, Chem. Mater. 14 (2002) 2910.
[3] G. Dantelle, M. Mortier, D. Vivien, G. Patriarche, Chem. Mater. 17 (2005) 2216.
[4] S. Sivakumar, F.C.J.M. van Veggel, M. Raudsepp, J. Am. Chem. Soc. 127 (2005) 12464.
[5] G. Blasse, B.C. Grabmaier, Luminescent Materials, Springer, Berlin, 1994.
[6] W. Lenth, R.M. Macfarlane, J. Lumin. 45 (1990) 346.
[7] P. Xie, S.C. Rand, Opt. Lett. 15 (1990) 848.
[8] J.P. Jouart, M. Bouffard, G. Klein, G. Mary, J. Lumin. 60-61 (1994) 93.
[9] U. Rambadu, T. Balaji, S. Buddhudu, Mater. Res. Bull. 30 (1995) 891.
[10] U. Rambabu, T. Balaji, K. Annapurna, S. Buddhudu, Mater. Chem. Phys. 43 (1996) 195.
[11] U. Rambadu, A. Mathur, S. Buddhudu, Mater. Chem. Phys. 61 (1999) 156.
[12] S. Areva, J. Holsa, R.-J. Lamminmaki, H. Rahiala, P. Deren, W. Strek, J. Alloys Compds. 300–301 (2000) 218.
[13] N. Imanaka, K. Okamoto, G. Adachi, Angew. Chem. Int. Ed. 41 (2002) 3890.
[14] N. Imanaka, K. Okamoto, G. Adachi, Chem. Lett. (2001) 130.
[15] M.S. Whittingham, A.J. Jacobson, Intercalation Chemistry, Academic Press, New York, 1982.
[16] E. Garcia, J.D. Corbett, J.E. Ford, W.J. Vary, Inorg. Chem. 24 (1985) 494.
[17] J. Holsa, L. Niinisto, Thermochim. Acta. 37 (1980) 155.
[18] E.A. Fidancev, M.L. Blaise, P. Porcher, J. Holsa, Evolution of Crystal Field effects in REOCl Series in Rare-Earth Development and Application, vol. 1, Academic Publishers, PR China, 1991, p. 95.
[19] J. Holsa, E. Sailynoja, K. Koski, H. Rahiala, Powder Diff. 11 (1996) 129.
[20] H. Mcmurdie, M. Morris, E. Evans, B. Paretzkin, W. Wong-Ng, C. Hubbard, Powder Diff. 1 (1986) 90.
[21] J. Holsa, P. Porcher, J. Chem. Phys. 75 (1981) 2108.
[22] O.V. Manoilova, S.G. Podkolzin, B. Tope, J. Lercher, E.F. Stangland, J.M. Doupil, B.M. Weckhuysen, J. Phys. Chem. B 108 (2004) 15770.
[23] S.G. Podkolzin, O.V. Manoilova, B.M. Weckhuysen, J. Phys. Chem. B 109 (2005) 11634.